KINEMATICAL RELATIONS BETWEEN WIND AND PRECIPITATION DISTRIBUTIONS

By Edwin Kessler, III

Geophysics Research Directorate, Air Force Cambridge Research Center

(Manuscript received 4 February 1959)

ABSTRACT

If distributions of precipitation in the atmosphere could be understood in terms of their associated three-dimensional winds, then radar, radiosonde, and surface observations might be utilized in new ways as sources of information about the winds. In this paper, continuity equations for precipitation content of the air are derived, and particular solutions are presented which give the vertical distribution of precipitation content where horizontal advection terms are small. These solutions apply to centers of widespread, horizontally uniform updrafts, or to the cores of simple cells such as represented by showers formed in the absence of vertical wind shear. A parabolic profile of updrafts is assumed. When the precipitation profile is steady-state and the fall speed of precipitation is constant, the amount of precipitation per unit volume of air increases rapidly downward in mid-atmosphere. Near the surface, changes in the vertical are very small. Maxima of precipitation content occur aloft before steady conditions obtain throughout the updraft layer; in the steady case, maxima aloft may occur when the terminal fall speed of precipitation increases during descent. The steady precipitation rate at ground level at centers of updraft regions may be significantly greater than the rate of condensation directly above, particularly when precipitation particles fall only slightly faster than the updrafts and with little increase of fall speed during their growth, as is often the case with snow. An explanation is offered for the difference between the vertical distributions of precipitation associated with widespread systems and with showers, and means for practical utilization of the results are suggested.

1. Introduction

The manner in which water substance is distributed in the atmosphere by the three-dimensional winds is of great meteorological interest. Insofar as accurate predictions of the winds can be made, knowledge of the accompanying distributions of condensed water depends largely on studies of kinematic relations between wind and atmospheric water. On the other hand, maps of the distribution of radar weather echoes used with records of radiosondes and rain gauges might be a source of new knowledge about the wind fields accompanying precipitation if relations between patterns of wind and precipitation were better known.

The following gives first results obtained from a study of continuity equations for water substance. Previous related work has followed several lines. Bannon [1] and others have computed the steady precipitation rate at various levels by assuming equality with the vertically integrated condensation above. This assumption is valid when there is no horizontal advection, and the vertical air velocity is much smaller than the fall speed of precipitation. Wexler and Austin [15] were concerned primarily with vertical distributions of radar reflectivity in widespread steady snow. Their derivations, applicable when updrafts are unvarying with height, are good representations of such profiles in the middle atmosphere. Wexler and Atlas [16] considered the role of various cloud-physics processes in establishing a balance between the cloud water which shares the motion of the air and precipitation which falls relative to the air. Their results apply in the widespread steady case when the updraft speed is small compared to the fall speeds of most of the precipitation. The present study differs from those mentioned above in that it neglects cloud-physics processes to derive vertical distributions of precipitation rate and precipitation water content in time-dependent and steady cases, and it is applicable to updrafts variable with height and a wide range of relations between updraft and precipitation falling speed.

2. The basic equations

M is here defined to be the amount by which the density of water, in all its phases, exceeds the saturation vapor density. When M is positive, it refers to the mass of condensed water substance per unit volume of air; when it is negative, it is the amount by which the saturation vapor density exceeds the actual. Following a development similar to that given by Haurwitz [7], for example, the equation of continuity for M can be written as follows:

$$\frac{\partial M}{\partial t} = -M\left[\frac{\partial(w+V_t)}{\partial z}+\frac{\partial u}{\partial x}+\frac{\partial v}{\partial y}\right] - (V_t+w)\frac{\partial M}{\partial z} - u\frac{\partial M}{\partial x} - v\frac{\partial M}{\partial y} + wG. \quad (1)$$

The terminal fall velocity of M relative to the air is V_t, always a negative number when M is positive. When M is zero or negative, V_t is zero, for the motion of M is then with the air in all respects. The x, y, and z (upward) wind components are denoted by u, v, and w, respectively, and G is a generation term which denotes the amount of water condensed from a unit volume of saturated air per unit vertical distance of air travel. This equation takes no account of the numerous processes of cloud physics which in nature affect the development of particles of M and prevent the occurrence of uniform V_t at a given level, as specified here. The presence of cloud water with precipitation is ignored. Although evidence is cited below to show that these omissions are unlikely to alter significantly the conclusions of this paper, (1) is still only an approximation to reality.

A means for rewriting (1) in a more useful form is provided by the equation of continuity for air,

$$\frac{\partial \rho}{\partial t} = -\left[u\frac{\partial \rho}{\partial x} + v\frac{\partial \rho}{\partial y} + w\frac{\partial \rho}{\partial z}\right] - \rho\left[\frac{\partial u}{\partial x} + \frac{\partial v}{\partial y} + \frac{\partial w}{\partial z}\right], \quad (2)$$

where ρ is the air density. In the real atmosphere, the local time change of density and the terms involving horizontal density variations are one to two orders of magnitude smaller than the other terms in (2). In this study, these terms are omitted, and the atmospheric motions are assumed to be governed by the relation

$$\frac{\partial u}{\partial x} + \frac{\partial v}{\partial y} + \frac{\partial w}{\partial z} = -w\frac{\partial \ln \rho}{\partial z}. \quad (3)$$

Substitution of (3) into (1) yields

$$\frac{\partial M}{\partial t} = -u\frac{\partial M}{\partial x} - v\frac{\partial M}{\partial y} - (V_t + w)\frac{\partial M}{\partial z} - M\left[\frac{\partial V_t}{\partial z} - w\frac{\partial \ln \rho}{\partial z}\right] + wG. \quad (4)$$

The derivatives of the wind appearing in equation (1) do not appear in the simpler relation, (4). This equation describes the local change of M in terms relating horizontal and vertical advection, divergence due to changes of terminal fall velocity with height, and condensation in rising air or evaporation in descending air. The term $Mw(\partial \ln \rho/\partial z)$ accounts for the compressibility of the atmosphere.

Equation (4) is a kinematic relationship and is the basic equation of this study. Meaningful solutions can be obtained by substituting for u, v, w, V_t, and G, values applicable to the atmosphere. By itself, (4) expresses no dynamical principles other than those implicit in the simplified form of the equation of continuity for air that has been used. General thermodynamic relations and cloud-physics processes could be accounted for in principle by a number of various equations applied simultaneously. This, however, is a problem for the future.

3. Simplified one-dimensional case

General forms of (4) can be solved by finite difference techniques. In this initial study, however, we are concerned with one-dimensional forms of (4). These are used to determine how the vertical distribution of M develops in the presence of a given wind field without horizontal advection of M. The explicit solutions are applicable to the centers of regions of low-level convergence in the atmosphere, where the horizontal advection terms are small. The one-dimensional solutions have additional implications pertaining to the two- and three-dimensional problems.

The one-dimensional equation without the product terms in M is amenable to exact treatment and shows the important properties of the one-dimensional solutions quite well. In this case, where

$$\frac{\partial M}{\partial t} = -(V_t + w)\frac{\partial M}{\partial z} + wG, \quad (5)$$

particles fall everywhere at constant speed relative to the air, and the atmosphere is incompressible. The closest analogy in the real atmosphere is the case of snow, for the terminal falling speed of snow particles increases (approximately) only as the cube root of the particle diameter [12]. Equation (5) relates the growth of M packets at a rate $dM/dt = wG$ to their descent at a rate

$$\frac{dz}{dt} = V_t + w. \quad (6)$$

With $\partial M/\partial t = 0$ in (5), substitution of the chosen wind field and boundary condition and integration between appropriate limits of z yield the corresponding steady-state solution. The parabolic vertical-velocity profile is a reasonable first approximation to conditions in the real atmosphere [4]; other complicated distributions can be approximated by a number of different parabolas. With $w = bz - az^2$, where a and b are constants, w is zero at $z = 0$ and $z = b/a$; its maximum value is $b^2/4a$ at $z = b/2a$. The boundary condition $M = 0$ at $z = b/a$ expresses the assumption that water substance does not enter the updraft region from above and that water saturation exists at the top of the updraft region. In the cases of a severe winter storm and a hurricane, a linear decrease of the generation function with increasing height has been found to be a very good approximation, and we take $G = A - Bz$. With these conditions, $M(z)$ is given by integrating from the top of the updraft region as follows:

$$M_z = \int_{z=b/a}^{z} \frac{(bz - az^2)(A - Bz)\,dz}{bz - az^2 + V_t} \tag{7}$$

and

$$M_z = -\frac{Bz^2}{2} + Az - \frac{BV_t}{2a}\ln(az^2 - bz - V_t) - \frac{V_t(bB - 2aA)}{a(-4aV_t - b^2)^{\frac{1}{2}}}\tan^{-1} \times \frac{2az - b}{(-4aV_t - b^2)^{\frac{1}{2}}}\Bigg|_{z=b/a}^{z}. \tag{8}$$

Equation (8) has been plotted for selected values of the constants. The family of full curves illustrated in fig. 1 refers to the case where $B = 0$ (*i.e.*, $G = A$) and shows steady-state conditions with the upper boundary condition $M = 0$. The dashed curve shown for the case $V_t = -b^2/2a$ is computed for $G = 2A(1 - az/b)$, in which the average value of G indicated on the abscissa is the same as the constant value taken previously. When $-V_t \leq w_{\max}$, the steady distributions of M are not defined, for elements of M are then trapped aloft and grow indefinitely.

The curves of fig. 1 show the amounts by which packets of M grow in falling from any level to any other level. Time-dependent solutions can be determined from any one of these plots with the aid of a corresponding graph that shows the time spent by M-packets in falling. The latter-type curve is obtained from the solution of equation (6) as follows:

$$t = \frac{2}{(-4aV_t - b^2)^{\frac{1}{2}}}\tan^{-1}\frac{2az - b}{(-4aV_t - b^2)^{\frac{1}{2}}}\Bigg|_{z}^{b/a}. \tag{9}$$

Fig. 2 shows this function for various values of V_t. The M packet arriving at any time, t, at the level at which solutions are desired has descended from an upper level given directly by fig. 2. The growth of the packet in this height interval is given by the curve of fig. 1 for corresponding V_t. If $M = 0$ at the initial time, then the value of M at the point and time in question is simply this growth increment. Fig. 3 shows distributions at various times which have been derived from accurate plots of the curves shown in figs. 1 and 2 for the case $V_t = -b^2/a$ and for the initial condition $M = 0$, corresponding to water-saturated air everywhere. If the vertical drafts suddenly cease, the subsequent M-profiles are given by downward displacement at speed $V_t = -b^2/a$ of the profile existing at time of cessation. Incidentally, it should be noted that exact time dependent solutions in a compressible atmosphere cannot be determined as shown above, for dM/dt is there a function of M.

4. Discussion of solutions

With G = constant, equation (5) and fig. 1 show that maximum downward increase of M in the steady case occurs in mid-atmosphere where updrafts and the condensation rate are also largest. When G increases downward, the maximum downward increase of M is shifted somewhat below the midpoint of the updraft layer. At the top and base of the layer where updrafts and condensation are zero, the vertical change of M in the steady case is also zero.

Changes of M are proportionately very small near the ground or base of the updraft layer. Consider, for example, that b/a = 30,000 ft. Then, in the layer from 10,000 ft to the base, in the case where $V_t = -b^2/a$ and G is constant, M increases by a factor of only 1.23. In the layer below 5000 ft, the increase is only 1.05. For typical precipitation, the radar reflectivity is about proportional to M^2, and so the corresponding reflectivity variations are near 1.8 and 0.4

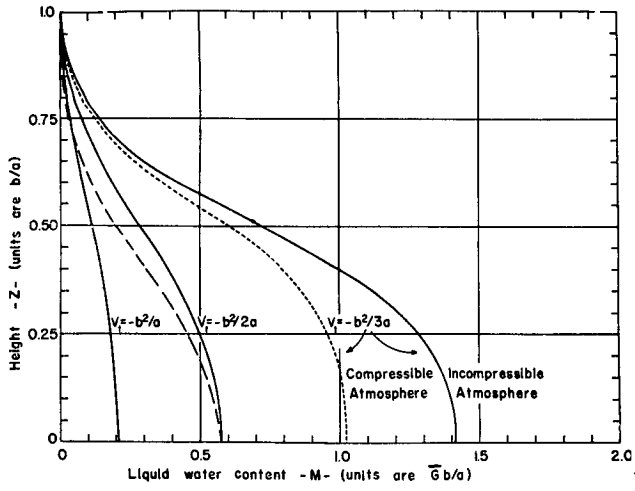

FIG. 1. Full curves show steady vertical profiles of water content for indicated values of constant fall speed, vertical velocity $w = bz - az^2$, constant generating function G, and an incompressible atmosphere. The dashed line is computed for $G = 2A(1 - az/b)$, where the average value of G, $\bar{G}$, is the same as the constant value used in the other curves. The dotted line shows the solution for constant G and a compressible atmosphere with b/a corresponding to about 10 km.

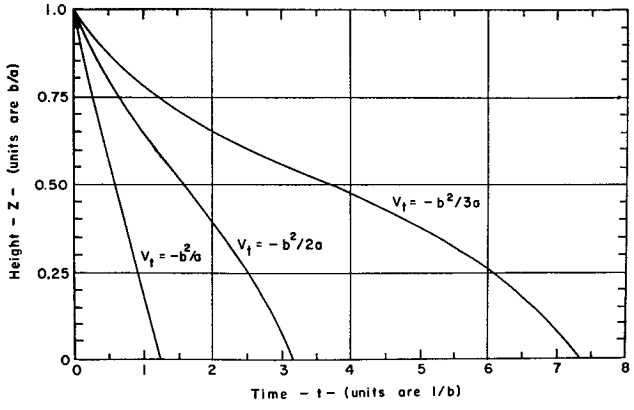

FIG. 2. Distance fallen against time for elements of water substance with indicated terminal speeds and updrafts $w = bz - az^2$.

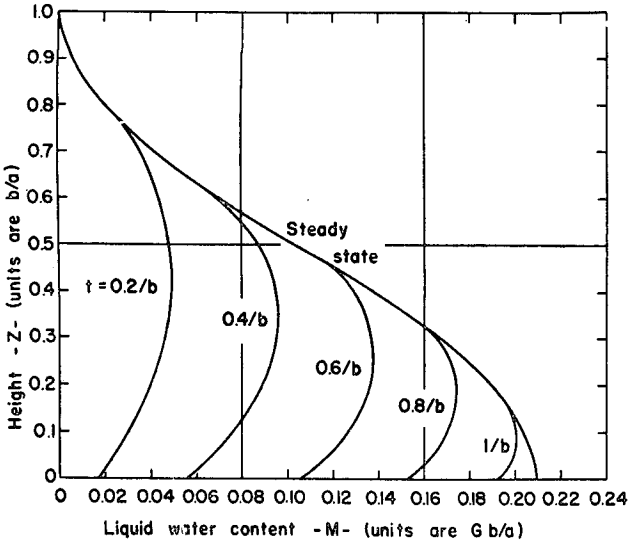

FIG. 3. Time dependent solutions of equation (5) discussed in the text. Terminal falling speed is $V_t = -b^2/a$.

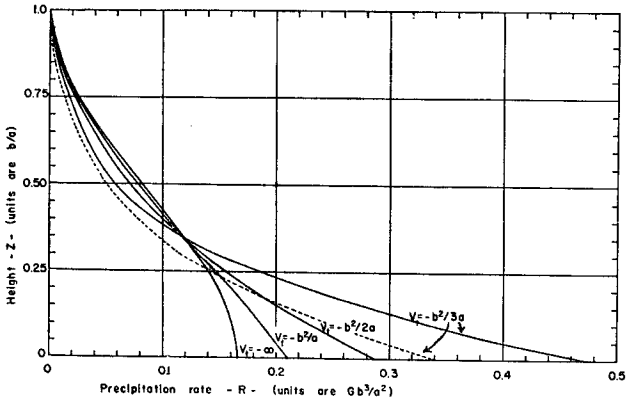

FIG. 4. Steady vertical profiles of precipitation rate. The curve labeled $V_t = -\infty$ is based on an identity between the precipitation rate at any level and the integrated condensation above. The others are derived from fig. 1 as discussed in the text.

db,[1] respectively. Slightly greater increases near the updraft base characterize the case of downward increase of G; the proportional changes near the base tend to be smaller for slower fall speeds, as can be deduced from the diagram. Wexler and Atlas' study [16] shows that the distribution of precipitation growth, when conditions are steady, is determined mainly by the updrafts and very little by the cloud-physics processes neglected here. Therefore, it appears that the results given here constitute an explanation of the observations of Harper [6] and Rogers [14] who report very small vertical variations of reflectivity in low levels during widespread uniform precipitation. In addition to this correspondence between theory and observation, a striking similarity exists between the entire curves of fig. 1 and average reflectivity profiles determined by the author during a case of widespread precipitation [8, p. 78]. The present work might, therefore, be considered an explanation of general features of the vertical M- or reflectivity distributions observed during such conditions. The work illustrates how a persistent, widespread layer in which M decreases with height might be related to updrafts and how the base of such a layer might be related to horizontal convergence in the wind field.

As shown by fig. 3, the maximum value of M occurs aloft before the M-distribution is steady. The maximum is initially where the rate of condensation (wG) is largest. Thereafter, M increases at each level until the vertical advection associated with its distribution balances the condensation rate there. With steady conditions, M-maxima aloft can occur if the precipitation particles increase their falling speed rapidly during descent, as illustrated in part 7b, below.

5. Steady vertical distribution of precipitation rate

The precipitation rate is given by

$$R = -M(V_t + w) \tag{10}$$

and its steady vertical distribution in this problem is therefore given by the curves of fig. 1 multiplied by corresponding values of $(V_t + w)$. The R-distributions shown in fig. 4, except for the curve labeled $V_t = -\infty$, are derived in this way.

When $|V_t| \gg |w|$, the terms Mw in (10) and $w(\partial M/\partial z)$ in (5) may be omitted. With constant fall speed of M, it follows from (10) that $\partial R/\partial z = -V_t(\partial M/\partial z)$. The result,

$$\frac{\partial R}{\partial z} = -wG, \tag{11}$$

applicable when $|V_t| \gg |w|$ and when horizontal advection of M is small, follows immediately from substitution of this differentiated form of (10) into (5) with $\partial M/\partial t$ and $w(\partial M/\partial z)$ omitted. The same result can be derived when vertical changes of V_t are considered, provided that $|V_t| \gg |w|$ everywhere. The curve in fig. 4 labeled $V_t = -\infty$ is computed from the integral of equation (11) to be

$$R_z = \int_z^{z=b/a} wG\,dz. \tag{12}$$

It is obvious from fig. 1 that large fall speeds are associated with small M's (updrafts remaining the same). Equation (10) shows that these associated tendencies in M and V_t tend to counteract one another as far as R is concerned. That the counteraction is not complete is shown by fig. 4, which indicates that, with

[1] Db (decibels) are cited here because of their widespread use by radar meteorologists. The difference between two quantities in db is ten times the logarithm of their ratio.

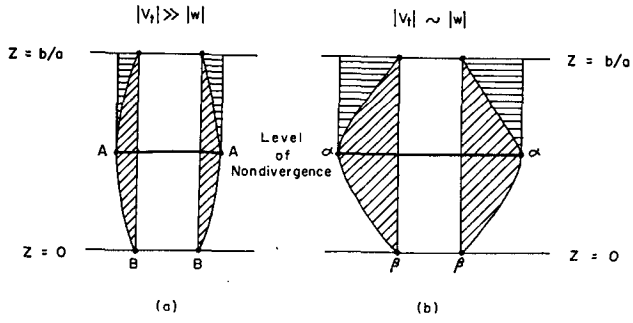

FIG. 5. Horizontal divergence in the high atmosphere, accompanying rising motion, spreads precipitation packets horizontally as they descend. The packets are contracted again by horizontal convergence in the lower atmosphere. The atmospheric volume contributing to precipitation at a section of the earth's surface is then larger than that vertically above by an amount suggested by the diagonally shaded areas in this diagram. Further discussion is in the text.

updrafts remaining the same, the precipitation rate tends to be smaller at the level of non-divergence and larger at the surface or base of the updraft layer as the precipitation fall speeds become smaller. This relation between the vertical distribution of precipitation rate and particle fall speeds is of fundamental importance to this study.

Fig. 5 illustrates schematically the physical basis of this relation through a comparison of the regions contributing to precipitation at the ground for two extremes of precipitation fall speed. When the precipitation falls much more rapidly than the updrafts, the horizontal divergence associated with the vertical-velocity distribution and implicit in equations (4) and (5) has little time in which to change the horizontal area of the M-packets. In this case, the region of diagonal shading plus the unhatched area in fig. 5a, all of which contribute to precipitation at section B–B on the ground, is only slightly larger than the unhatched area alone. The latter is presumed to be all that contributes to surface precipitation when equation (12) is used. When the M-packets fall slowly, however, they are horizontally spread a great deal above the level of non-divergence and contracted horizontally below. The volume contributing to precipitation at a section of the ground is then much larger than is contained vertically above that section, and the surface precipitation rate is accordingly larger than the result given by (12).

At the level of non-divergence, on the other hand, the volume contributing to precipitation is less than it is vertically above any given cross section at that level. The amounts by which the precipitation rate at the level of non-divergence falls short of the amounts predicted by (12) are suggested by comparison of the horizontally hatched areas above segments A–A and α–α in fig. 5 with the total area vertically above these lines.

Since this model, which applies where the horizontal advection of M is zero, predicts more precipitation at the ground and less at the level of non-divergence than is created directly above those levels, it implies the major features of the water distributions of two- and three-dimensional wind-field models, which are required in order to satisfy conservation principles. The level of non-divergence and higher levels in the analogous two- or three-dimensional cases are characterized by precipitation or water substance spread over a horizontal area larger than that containing updrafts, while precipitation at the ground is confined to a smaller area. Real counterparts of this picture are suggested by the anvil shapes of thunderstorms and the cloud and precipitation distributions of widespread storms.[2]

6. Numerical example

While it is planned to calculate numerical values appropriate to various weather situations and varying terminal falling speeds at another time, a brief introduction of this is given here. The curves in fig. 1 drawn for $V_t = -b^2/2a$ may be referred to a fall speed of 1 m per sec, corresponding approximately to the fall speed of snowflakes. The value of w_{max} is then 50 cm per sec, a value found in association with the most intense of general storm systems. In a storm extending to 10 km or 30,000 ft, the corresponding values of a and b are 2×10^{-8} m^{-1} sec^{-1} and 2×10^{-4} sec^{-1}, respectively. The generating function is given from considerations of the temperature distribution and is most easily computed by reference to a pseudo-adiabatic diagram or one such as Fulks' [5]. For a case where the temperature ranges around 0C to −10C from the surface to 700 mb and at higher levels follows the moist adiabatic lapse rate to 300 mb, G is nearly given by $1.67 \times 10^{-3}\,(1 - 10^{-4}\,z)$ g per m^4. The steady state value of M at the ground is then (from fig. 1) $0.58\ \bar{G}b/a$ or 4.8 g per m^3 and the precipitation rate there is $-MV_t = 4.8$ g per m^2 sec or 17.4 mm per hr. When the value $V_t = -b^2/a$ is referred to fall speeds of 1 m per sec, the associated maximum updraft is 25 cm per sec, the water content of the air at the ground is 1.7 g per m^3, and the precipitation rate there is 6.3 mm per hr.

The precipitation rate with 50 cm per sec maximum updraft corresponds to about 7 in. per hour, unmelted, and is probably about equal to or greater than the maximum snowfall rate ever observed in connection with widespread storms. The updrafts in this case in the middle atmosphere are, in fact, about equal to the fall velocity of the single snow crystals that would

[2] When there is unsaturated air, of course, much condensed water may be re-evaporated while descending to the ground. Quantitative evaluation of this is implicit in solutions of bounded two- and three-dimensional models. See section 7e, below, and [10].

TABLE 1. Distribution of M in cases of discontinuous increase of V_t. In each case, $W_{max} = 0.25\ b/a$.

Case I					Case II					Case III				
z (b/a)	V_t b^2/a	V_t+w b^2/a	M Gb/a	R Gb^3/a^2	z	V_t	V_t+w	M	R	z	V_t	V_t+w	M	R
1	−1	−1.000	0	0	1	−0.5	−0.500	0	0	1	−0.333	−0.333	0	0
0.5	−1	−0.750	0.104	0.078	0.5	−0.5	−0.250	0.285	0.071	0.5	−0.333	−0.083	0.709	0.059
0.5	−5	−4.750	0.016	0.078	0.5	−2.5	−2.250	0.032	0.071	0.5	−1.667	−1.417	0.042	0.059
0	−5	−5.000	0.034	0.169	0	−2.5	−2.500	0.068	0.170	0	−1.667	−1.667	0.099	0.164

really exist there when temperatures are low enough to allow snow at the ground. When updrafts are of the same order as particle falling speeds, the particles will not fall to the ground except as they grow and increase their speed or are carried horizontally to a place where updrafts are less. It appears unlikely that precipitation-rate increases rapidly with updrafts beyond the intensity where a major fraction of the particles cannot descend through those same intense updrafts to the ground. In this case, the snow should be dispersed over a great horizontal area, much of it evaporating in downdrafts before reaching the ground. The distribution of precipitation rate is thus related to aspects of particle mechanics and dynamics which determine particle falling speeds, as well as to other aspects of cloud physics and to the updrafts.

7. Extension of work

(a) *Compressibility of the atmosphere.* The term $Mw(\partial \ln \rho/\partial z)$ in (4) accounts for the compressibility of the atmosphere and is most important in thick layers and when V_t is small. Inclusion of this term greatly complicates formal solution of the equation, but answers can be readily obtained by finite-difference methods. With $b/a = 30{,}000$ ft, the ARDC Model Atmosphere 1956 [13] shows $\partial \ln \rho/\partial z = -0.477$, nearly independent of z. In the numerical work leading to the results given here, $\partial \ln \rho/\partial z$ was taken as -0.5. The dashed lines in figs. 1 and 4 show the result of this consideration of compressibility for the steady case where $V_t = -b^2/3a$. The difference between the simpler model and this one becomes smaller for smaller values of M (faster fall speeds) and is trivial for $V_t = -b^2/a$. It is clear that effects of compressibility do not change the general conclusions reached above regarding the distribution of growth.

(b) *Variable V_t.* A prominent variation of V_t which can be easily considered is given by the case of snow melting to rain. Usually, the melting takes place in a zone about 1000 ft thick, accompanied by some growth in the interval and by a fivefold increase of terminal falling speed, approximately. In the present model, a discontinuous change of V_t is assumed, and solutions are obtained by making use of the equality of precipitation rates on both sides of the V_t transition. Table 1 gives results for three velocity regimes in an incompressible atmosphere, with constant generation function and with change of V_t at the level of non-divergence.

Since M is reduced upon melting according to the change of $V_t + w$, instead of V_t, this decrease of M is always a greater proportion than the proportional increase of V_t. This is especially true when the magnitude of V_t in the snow barely exceeds the updrafts, as in case III. The values of M and R after melting are always less than those which would exist if the M-packets were to descend all the way from the upper boundary with their melted velocity. This is consistent with continuity considerations because during the history of slow fall, horizontal divergence spreads M laterally to a greater extent than otherwise and this history, implicitly accounted for by the equations, is unaffected by a sudden change of V_t. The integrated effects of high-level horizontal divergence are, of course, brought to the surface and through the lower region of horizontal convergence more quickly when there is an increase of falling speed. In such a case, precipitation arriving at the ground is spread over a larger area more characteristic of the upper level where speedup occurs, and precipitation at the ground is correspondingly reduced in intensity. The least surface precipitation rate at the center of an updraft region occurs when the terminal speed of falling particles increases at the level of non-divergence, where the cumulative effects of horizontal divergence are a maximum. The precipitation rate at the level of non-divergence may be quite small, as suggested by fig. 4, when the fall speed above only slightly exceeds the updrafts. With large fall speeds below that level, the precipitation rate would increase only at about the relatively slow rate given by the curve for $V_t = -\infty$ in fig. 4. The physical basis of most of these statements can be readily appreciated from illustrations similar to fig. 5. When fall speeds are variable, such diagrams are not symmetrical about the level of non-divergence.

During accretion of supercooled cloud drops or rapid growth, the fall speed of growing M-packets might increase so rapidly that an upper layer of high M is produced even without melting. Determination of radar-reflectivity profiles associated with such changes of fall speed requires consideration of small-scale proc-

esses, including the interactions among the particles which characterize real rain or snow samples.

(c) *Two and three dimensions.* Certain features of the two- and three-dimensional cases may be deduced directly from the work reported here. It is especially interesting to contrast the situations prevailing in relatively small-scale phenomena where updrafts are of the same order as the fall velocity of precipitation particles and large-scale phenomena where updrafts are much less. In the former case, analogous to thundershowers, the precipitation maximum aloft, characteristic of the initial stages, descends so slowly that it cannot reach the ground before appreciable low-level horizontal convergence and accompanying advection of drier air from the surroundings or downdraft portion of the cell have occurred. In this case, the precipitation has a high intensity in a small area at the surface but also undergoes extensive evaporation elsewhere in the low levels while it falls from the widespread anvil cloud above. Great amounts of condensed water aloft are associated with the strong updraft of the storm center. This, in part, may explain observations of Chmela and Donaldson of vertical profiles of radar reflectivity in thunderstorms, where pronounced maxima aloft are often noted [2; 3]. On the other hand, when updrafts are of large horizontal extent and fall speeds are large compared to the updrafts, steady-state profiles such as shown in fig. 1 may prevail for a long time over a relatively large area and only near the edges of the updraft area depart greatly from the model distributions given here.

(d) *Computation of vertical-air-velocity profiles in real cases.* In practice, water-content distributions (as deduced from radar data, for example) can be a basis for deduction of the wind field. Estimates of steady vertical-velocity profiles, when there is no horizontal advection of M, are feasible with today's knowledge and observational data. Absence of horizontal advection is probably a good assumption when radar echoes are locally steady and horizontally uniform. In this case, it is practicable to compute w at closely spaced intervals along the vertical profiles of M from the equation

$$w = \frac{\frac{\Delta}{\Delta z}(MV_t)}{G + \frac{\Delta M}{\Delta z} + M\frac{\Delta \ln \rho}{\Delta z}} \qquad (13)$$

which is similar to equation (4). Here, M and V_t and their derivatives would be derived from the radar data, and G and ρ would be derived from radiosonde ascents or climatological records. The nature of the known relations between radar reflectivities, M, and V_t will not generally permit conclusions that particular vertical-velocity profiles actually occur. However, the use of equation (13) or similar relations with dynamical equations and other data, such as surface rainfall rates, serves to constrain the range of possible answers and, as already reported [8], definitely assists delineation of the field of motion accompanying precipitation. Application of the new results given here in studies of the real atmosphere is proceeding with the aid of recently developed techniques which allow rapid quantitative mapping of radar echoes [9; 11].

(e) *The future.* General extension of the present work requires use of finite-difference techniques, and large digital computers are being used to obtain solutions of two-dimensional atmospheric models, incorporating various wind fields. In these cases, negative values of M may occur as initial or boundary conditions and are generated in the downdrafts. It is hoped to include dynamical considerations in the work eventually, as well as aspects of the small-scale processes concerning development of precipitation from cloud particles. In addition to relating water distributions and radar-echo patterns to the wind field, we are interested in learning of the interaction of parameters which determine the amount and distribution of water precipitated during convection.

8. Summary

In this study of the distribution of precipitation in the atmosphere, the precipitation content of a unit volume of air is related to the field of motion. Vertical profiles of water content are derived for a parabolic vertical-velocity profile with no horizontal advection of water. These are in good agreement with radar observations of water distributions observed in widespread storms. The differences between radar-reflectivity or precipitation profiles observed in the disparate cases of widespread cyclonic storms and thunderstorms are qualitatively explained in terms of the interactions between updrafts, precipitation fall speed, and horizontal advection characteristic of the cases.

The precipitation rate approximates the integrated condensation rate over a unit cross section at the center of a widespread updraft area when precipitation falling speeds are large compared to the updrafts. When fall speeds are constant, the surface precipitation rate at updraft centers in saturated air is always greater than that given by the integrated condensation above a unit cross section. Increasing fall speed of precipitation during downward descent, characteristic of most precipitation, effects a decreased precipitation rate at the ground from what would prevail otherwise. Decreasing fall speed, as might occur in the case of melting hail in thunderstorms, enhances the effects of low-level convergence to concentrate the surface precipitation over a small area. While this study treats a limited number of cases, it illustrates

some of the basic kinematic relations between wind and water fields and suggests means whereby radar and other meteorological instruments might be used to learn more of the general wind fields accompanying precipitation.

Acknowledgments. Dr. Raymond Wexler reviewed the basic derivations, and there were many valuable discussions with Dr. David Atlas and Mr. William Rogers. Mr. Rudolph Loeser and Mr. Ralph Newcomb prepared the illustrations.

REFERENCES

1. Bannon, J. K., 1948: The estimation of vertical currents from the rate of rainfall. *Quart. J. r. meteor. Soc.*, **74**, 57–66.
2. Chmela, A. C., 1958: *Reflectivity measurements in the vertical through a severe squall line.* Proc. 7th Wea. Radar Conf., Amer. meteor. Soc., Boston, Mass.
3. Donaldson, R. J., 1958: *Vertical profiles of radar reflectivity in thunderstorms.* Proc. 7th Wea. Radar Conf., Amer. meteor. Soc., Boston, Mass.
4. Fleagle, R. G., 1947: The fields of temperature, pressure, and three-dimensional motion in selected weather situations. *J. Meteor.*, **4**, 165–185.
5. Fulks, J. R., 1935: Rate of precipitation from adiabatically ascending air. *Mon. Wea. Rev.*, **63**, 291–294.
6. Harper, W. G., 1956: *Variation with height of rainfall below the melting level.* Proc. 6th Wea. Radar Conf., Amer. meteor. Soc., Boston, Mass.
7. Haurwitz, B., 1941: *Dynamic meteorology.* New York, McGraw Hill, 129–130.
8. Kessler, E., III, 1957: Radar-synoptic analysis of an intense winter storm. *Geophys. Res. Pap. No. 56*, GRD, AFCRC.
9. ——, 1958: *Use of radar in kinematical studies of precipitating weather systems.* Proc. 7th Wea. Radar Conf., Amer. meteor. Soc., Boston, Mass.
10. ——, 1958: *Fields of motion and temperature in hurricanes as revealed by radar.* Proc. Tech. Conf. on Hurricanes, Amer. meteor. Soc., Boston, Mass.
11. ——, 1959: The PAR-Scope: An oscilloscope display for weather radars. *IRE Trans. on Aeronautical and Navigational Electronics*, **ANE-6**, No. 1.
12. Langleben, M. P., 1954: The terminal velocity of snowflakes. *Quart. J. r. meteor. Soc.*, **80**, 174–181.
13. Minzner, R. A., and W. S. Ripley, 1957: ARDC Model Atmosphere 1956 (Chap. 1, Sect. 2, in *Handbook of Geophysics*). Cambridge, Geophys. Res. Dir., AFCRC.
14. Rogers, W., 1958: *Note on vertical variations in radar reflectivity.* Tech. Note No. 1 on Contract AF 19(604)–2291 between Geophys. Res. Dir. and Mass. Inst. Tech.
15. Wexler, R., and P. M. Austin, 1954: *Radar signal intensity from different levels in steady snow.* Res. Rep. No. 23, Wea. Radar Res., Dept. Meteor., Mass. Inst. Tech.
16. ——, and D. Atlas, 1957: Moisture supply and growth of stratiform precipitation. *J. Meteor.*, **15**, 531–538.